Proceedings of the ASME 2017 Internal Combustion Engine Fall Technical Conference
ICEF 2017
October 15-18, 2017, Seattle, Washington, USA

ICEF2017-3661 (DRAFT)

Influence of charge motion and compression ratio on the performance of a combustion concept employing in-cylinder gasoline and natural gas

James Sevik
Argonne National Laboratory
Lemont, IL

Michael Pamminger
Argonne National Laboratory
Lemont, IL

Thomas Wallner
Argonne National Laboratory
Lemont, IL

Riccardo Scarcelli
Argonne National Laboratory
Lemont, IL

ABSTRACT

The present paper represents a small piece of an extensive experimental effort investigating the dual-fuel operation of a light-duty spark ignited engine. Natural gas (NG) was directly injected into the cylinder and gasoline was injected into the intake-port. Direct injection of NG was used in order to overcome the power density loss usually experienced with NG port-fuel injection as it allows an injection after intake valve closing. Having two separate fuel systems allows for a continuum of in-cylinder blend levels from pure gasoline to pure NG operation. The huge benefit of gasoline is its availability and energy density, whereas NG allows efficient operation at high load due to improved combustion phasing enabled by its higher knock resistance. Furthermore, using NG allowed a reduction of carbon dioxide emissions across the entire engine map due to the higher hydrogen-to-carbon ratio. Exhaust gas recirculation (EGR) was used to (a) increase efficiency at low and part-load operation and (b) reduce the propensity of knock at higher compression ratios (CR) thereby enabling blend levels with greater amount of gasoline across a wider operating range. Two integral engine parameters, CR and in-cylinder turbulence levels, were varied in order to study their influence on efficiency, emissions and performance over a specific speed and load range. Increasing the CR from 10.5 to 14.5 allowed an increase in indicated thermal efficiency of more than 3% for 75% NG (25% gasoline) operation at 8 bar net indicated mean effective pressure and 2500 RPM. However, as anticipated, the achievable peak load at CR 14.5 with 100% gasoline was greatly reduced due to its lower knock resistance. The in-cylinder turbulence level was varied by means of tumble plates as well as an insert for the NG injector that guides the injection "spray" to augment the tumble motion. The usage of tumble plates showed a significant increase in EGR dilution tolerance for pure gasoline operation, however, no such impact was found for blended operation of gasoline and NG.

INTRODUCTION

The increasing availability and low price of NG compared to other petroleum bases fuels in the US are the main reasons for the growing interest in this energy carrier. As depicted in Figure 1, it is projected that the production of NG will continue to rise over the next few decades. NG, comprised mainly of methane, is very attractive for use in internal combustion engines. Transforming the vehicle fleet to NG fueled engines can reduce the operating costs and at the same time reduce dependency on crude oil. Furthermore, NG can be an enabler for meeting emissions (CO_2) regulations, which are becoming stricter over time. The methane molecule is very compact and has a molar hydrogen-to-carbon (H/C) ratio of four. In contrast, gasoline has a molar hydrogen-to-carbon ratio of approximately 1.8. A higher H/C ratio combined with a greater lower heating value (LHV) imply that by using NG instead of gasoline, and maintaining the same efficiency, the emitted CO_2 emissions can be reduced by 25%.

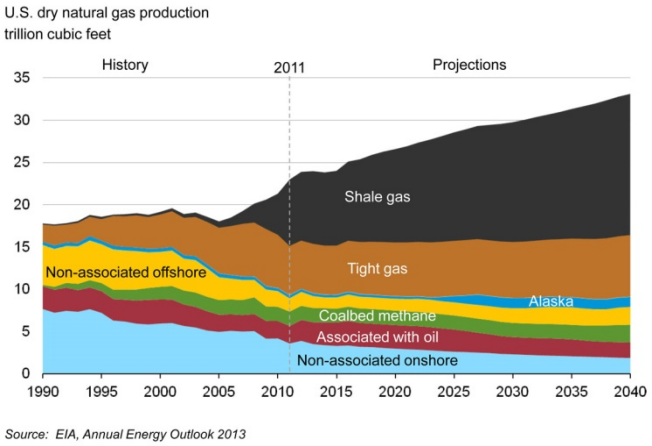

Figure 1: Historic and projected production of NG

The high stability of the methane molecule leads to a very high knock resistance, which enables engine operation at high load conditions even with higher CR. Engine operation with gasoline under similar conditions requires adoption of knock mitigation measures such as retarded ignition timing and fuel enrichment. These knock mitigation measures reduce engine efficiency and therefore increase fuel consumption. As it is gaseous under typical engine operating conditions, use of NG precludes some of the issues associated with liquid fuels such as evaporation, wall wetting and oil dilution. The aforementioned high stability of the methane molecule can be disadvantages in low load regions because of long combustion durations [1]. One disadvantage of using NG is the lower volumetric energy density. The range of the vehicle can be compromised relative to gasoline, due to limitations of tank size. Another disadvantage is the lower power density if NG is injected into the intake manifold, as it displaces air resulting in a lower volumetric efficiency. In order to overcome this, the engine in the current investigation was equipped with a NG direct injection (DI) system. DI can increase the volumetric efficiency if fuel is injected after intake valve closing (IVC), allowing the engine to aspirate as much air as possible, resulting in a power density increase.

In order to best utilize the properties of both fuels, this paper describes blended operation of NG and gasoline. The main aim of these experiments was to investigate the influence of CR and in-cylinder turbulence on EGR dilution at part-load. Additionally, the NG-gasoline blend required to mitigate knocking combustion under wide-open-throttle (WOT) conditions was of particular interest and was investigated at various engine speeds and CR.

EXPERIMENTAL BACKGROUND

Steady state experiments were conducted on a single cylinder research engine. The engine was equipped with port-fuel injection (PFI) for gasoline (E10) and central and side mounted DI for NG, as shown in Figure 2. For NG DI an outward opening injector was used. The side injector was located close to the intake valves and had a 60° angle relative to the cylinder axis and the central injector was located next to the spark plug Unique to this study was the usage of a fourth generation NG DI injector, supplied by Delphi [2]. This outward-opening solenoid injector allowed an injection pressure of up to 15 bar gauge pressure. The port fuel injector was delivered by Ford and was operated with an injection pressure of 4.1 bar. The paper includes comparisons of different energy based blend ratios of 25, 50, and 75% NG. The balance was covered by gasoline, which was injected into the intake port at -540 degree crank angle after top dead center (°aTDC firing). Investigations were done at part-load (with and without EGR dilution) as well as WOT. A Motec M800 engine control unit was used to control the ignition timing as well as the injection timing for both fuel systems. Specifications of the engine are listed in Table 1.

Combustion air was supplied by an Atlas Copco air compressor; throttling was achieved by using a Parker Pilot regulator in the intake stream. Fuel flows were measured using a Coriolis fuel meter CMF010 from Micro Motion for each fuel separately. Crank angle resolved data were recorded using an AVL 365X crank angle encoder. The physical resolution was 0.5°CA [3]; internal calculations from the AVL data acquisition system delivered 0.1°CA resolution for the crank angle based data. In-cylinder pressure data were measured with an AVL GU21C pressure transducer. The spark timing (ST) was adjusted as needed in order to maintain 50% of the integrated area (AI50) of rate of heat release (ROHR) at 8°aTDC, which corresponds to maximum break torque (MBT). A conventional ignition coil was used, with a nominal energy level of 75 mJ. For full load operation, retarded ignition was preferred over enrichment as a knock mitigating measure. Exhaust backpressure was held at ambient conditions.

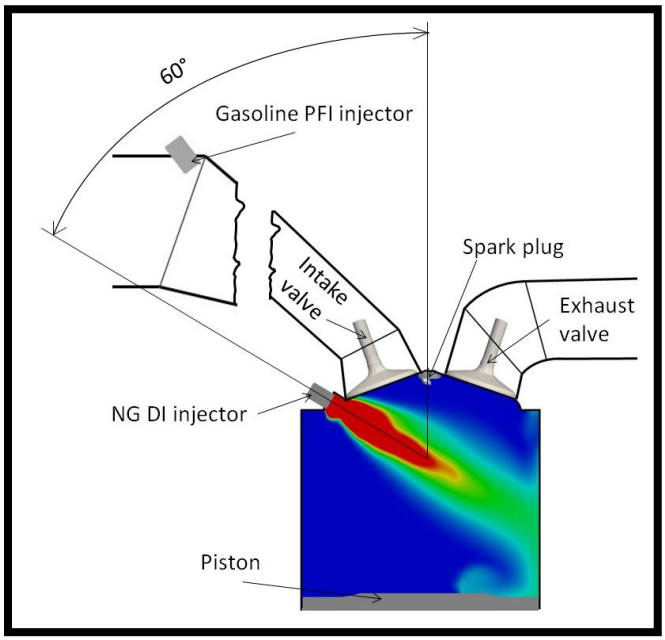

Figure 2: Schematic of the Engine Setup

Table 1: Engine Specific Parameters

Displacement [cm^3]	626.4
Stroke [mm]	100.6
Bore [mm]	89.04
Geometric Compression Ratio	10.5:1
Number of Intake/Exhaust Valves	2/2
Spark Plug	NGK, 0.7 mm gap
Tumble Ratio	0.6
Exhaust valve open/close [°aTDC fired]	150/-350
Intake valve open/close [°aTDC fired]	350/-140

The properties of E10 listed in Table 2 are representative of commercially available regular unleaded gasoline. The E10 was delivered from a regional distributor. The properties of NG in Table 2 represent the typical composition available from the NG pipeline. However, in order to ensure consistent NG composition, NG was delivered in cylinders from a regional distributor. The properties/ compositions shown in Table 2 were extracted from a certificate of analysis delivered by the distributor.

Table 2: Fuel Specifications for Gasoline (E10) and Natural Gas (NG)

Gasoline (E10)		Natural Gas (NG)	
C,H,O [wt%]	82.08,14.13,3.79	CH_4, $C2H_6$, CO_2, N2 [mol%]	94,3,2,1
LHV [MJ/Kg]	42.02	LHV [MJ/Kg]	46.93
AFRSTOICH [-]	14.1	AFRSTOICH [-]	16.2
AKI (R+M)/2	87		

Experimental Approach

Steady-state engine testing was performed for one part-load condition as well as WOT. For part-load operation, 1500 RPM 5.6 bar net indicated mean effective pressure (IMEP) was chosen as it is representative of road load conditions. Investigations were done with neat E10 and neat NG, as well as specific blend ratios of NG (25, 50 and 75%) on an energy basis. Stoichiometric operation was maintained for all operating points. High-speed data for each operating condition, which were measured three times in a row, are averaged over three times 375 cycles. The intake pressure was adjusted as needed in order to maintain the target IMEP. WOT tests were performed by adjusting the intake pressure to 14.5 psia. The operating conditions for part-load as well as WOT are summarized in Table 3.

Table 3: Experimental Matrix

Engine Speed [RPM]	1500
Load IMEP [bar]	5.6, WOT
SOI DI [°aTDC fired]	Sweep, -120 to -360
SOI PFI [°aTDC fired]	-540

EGR rates were calculated using equation (1) sampling CO_2 emissions from the intake and exhaust stream. In order to get representative EGR rates, the CO_2 concentration in ambient air was sampled twice daily. Raw emissions were sampled using a Pierburg AMA2000 emissions bench.

$$EGR = \frac{CO_{2_{intake}} - CO_{2_{ambient}}}{CO_{2_{exhaust}} - CO_{2_{ambient}}} \quad (1)$$

Combustion Metrics

Equation (2) represents the first law of thermodynamics applied on a closed system. By neglecting blow-by gases the time frame between IVC and exhaust valve opening (EVO) can be seen as a closed system. In order to determine the total heat release, equation (3) is used. Both equations are implemented within the data acquisition system and calculate the added fuel energy subtracted by the wall heat loss over crank angle. The gas properties are calculated based on the in-cylinder pressure. The gas properties of the in-cylinder mixture are described by γ; p is the in-cylinder pressure; V the in-cylinder volume and θ defines the crank angle.

$$\frac{dQ}{d\theta} = \frac{1}{\gamma - 1} \cdot \left(\frac{\gamma \cdot p \cdot dV}{d\theta} + \frac{V \cdot dp}{d\theta}\right) \quad (2)$$

$$AI = \int_0^{100} \frac{dQ}{d\theta} \cdot d\theta \quad (3)$$

The early flame development process is described by the flame development angle (FDA) which is defined as the difference in °CA between ST and AI10, shown in equation (4).

$$Flame\ Development\ Angle = AI10 - Spark\ Timing \quad (4)$$

The CD is used in order to describe the actual combustion process, which is defined as the difference in °CA from AI10 to AI90, shown in equation (5).

$$Combustion\ Duration = AI90 - AI10 \quad (5)$$

The coefficient of variance of IMEP (COVIMEP), defined in equation (6), was used in order to quantify the stability of the engine operation. A 3% limit was imposed for stable engine operation which was derived over three times 375 cycles. σ represents the standard deviation and μ the mean value.

$$\mathrm{COV_{IMEP}} = \frac{\sigma_{\mathrm{IMEP}}}{\mu_{\mathrm{IMEP}}} \quad (6)$$

RESULTS

INFLUENCE OF CHARGE MOTION ON EGR DILUTION TOLERANCE AND EFFICIENCY (CR 12.5)

The following three sections will focus on how changes to the in-cylinder charge motion will influence EGR dilution tolerance and resulting ITE. Changes to charge motion were accomplished by three hardware means: tumble plates, injector insert, and CR. The tumble plates act as port-blockers, causing an increase in tumble. An increase in CR will reduce the squish height, which increases turbulence due to the squish effect [5].

The custom made cylinder head allowed installation of the NG DI injector in two different locations: centrally mounted right next to the spark plug, side mounted between the head gasket and the intake valves with a 60° angle relative to the cylinder axis. Previous investigations [4] showed higher indicated thermal efficiency (ITE) for the operation with the NG DI injector in side location compared to the NG DI injector in central location. However, those investigations were performed without the insert in place in central location. In order words, the injector in central location was used in the same manner (without insert) Figure 3.

Three dimensional CFD simulation showed a significantly higher turbulence level at spark timing for the engine setup with the NG DI injector in side location relative to central injection [4]. With the objective of replicating the superior spray characteristics of the NG DI injector in the side location, an insert was designed for the central location to guide the spray. The insert transforms the injection event into an inward-opening configuration. The inset in Figure 3 shows the machined insert. The rendered cylinder head in Figure 3 depicts the insert in place ahead of the NG DI injector in central location, as well as the NG DI injector in side location (without the insert).

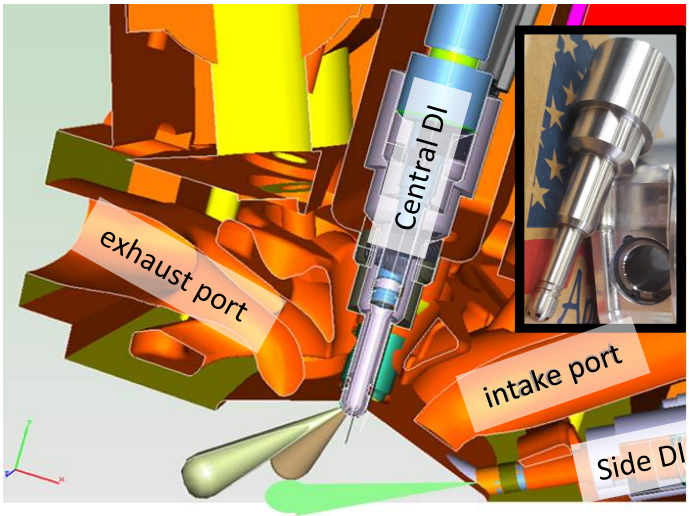

Figure 3: Cylinder Head Rendering

The insert was indexed to guide the injection spray towards the exhaust ports, with the goal of augmenting the tumble motion. Also illustrated in Figure 2 are the spray plumes from the NG DI injector in side location, which inherently enforced the tumble motion due to the alignment with the incoming mass flow during the aspiration process.

Engine Operation without Tumble Plates

Figure 4 shows the EGR dilution tolerance versus blend ratio for a COVIMEP smaller or equal to 3%. In Figure 4, 0% NG represents pure E10 operation and is influenced neither by the NG DI injection location nor by the insert, as it represents the injection of pure E10 in the intake port. The blue and the red circle at 0% NG show two different measurements at the same boundary conditions. The significant improvement observed in dilution tolerance for both configurations as the blend ratio increased from 0% to 25% NG is most likely due to the enhancement of the charge motion due to direct injection of NG, which in turn would be expected to speed up the combustion process.

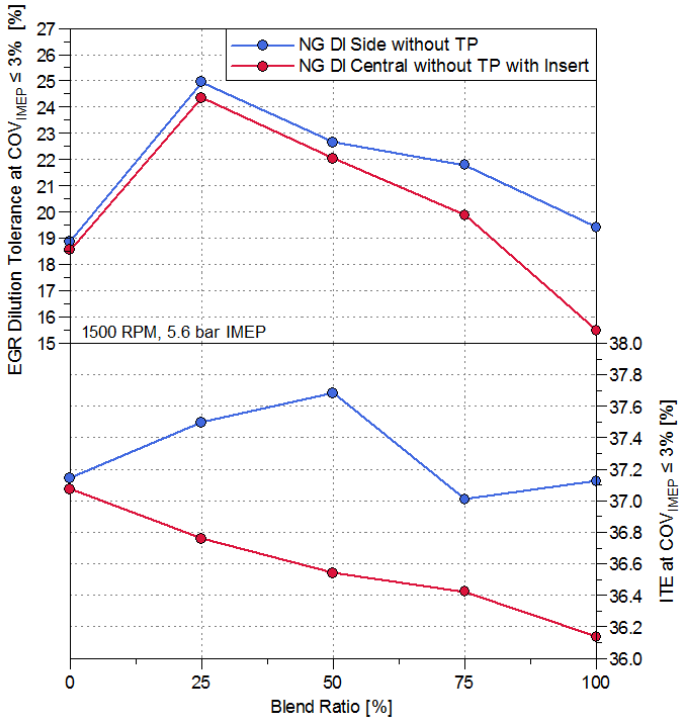

Figure 4: NG DI in Side Location vs NG DI in Central Location with Insert, 1500 RPM, 5.6 bar IMEP EGR Dilution Tolerance

The direct injection of NG might have increased the in-cylinder turbulence level and therefore sped up the combustion and increased the EGR dilution tolerance. However, as anticipated, by increasing the blend ratio beyond 25%, the EGR dilution tolerance decreased due to the lower laminar flame speed of NG compared to E10 [6]. As shown in Figure 4, at blend ratios of 25 and 50% NG, the EGR dilution tolerance for both configurations is similar. However, for 75 and 100% NG blend ratios a diverging trend is observed with a reduced EGR dilution tolerance for NG DI in central location. The difference

in the EGR dilution tolerance might have been caused by dissimilar fuel distribution and therefore differences in the combustion process.

The bottom plot of Figure 4 shows ITE versus blend ratio for the NG DI in side location and NG DI with the insert in central location. Pure E10 operation with an EGR dilution of about 19% showed an ITE of about 37.1%. The ITE for NG DI in central location decreases monotonically as the blend ratio is increased from 0 to 100% NG. The lowest efficiency measured for NG DI in central location was 100% NG with an efficiency of 36.1%. For the NG DI in side location, as the blend ratio increases, the ITE first rises with a peak value of 37.7% at 50% NG and then decreases. Increasing the blend ratio beyond 50% NG showed deteriorating EGR dilution tolerance and the efficiency leveled out at an ITE value close to pure E10 operation of about 37.1%. As discussed in the previous section, turbulence is crucial for not only a high dilution tolerance but also the fuel distribution. Literature has shown that an increasing in-cylinder turbulence can lead to increased heat transfer rates, which can be attributed to the loss in ITE [5].

In order to further understand the impact of fueling strategy on engine efficiency, ITE and COVIMEP were examined as a function of EGR rate for both the side (Figure 5) and central (Figure 6) NG DI locations. As the EGR rate was increased, the ITE was increased for all fueling strategies. Relative to blended operation, EGR dilution tolerance was lowest for neat fuels (E10 or 100% NG). However, increasing the NG blend ratio from 0% to 25% showed the most significant increase in EGR dilution tolerance. Beyond 25% NG, the EGR dilution tolerance decrease. Apparent is the effect of highest efficiency right about 3% COVIMEP. The ITE decreased if the EGR rate was further increased due to the decreasing stability of the combustion due to partial burns or misfire.

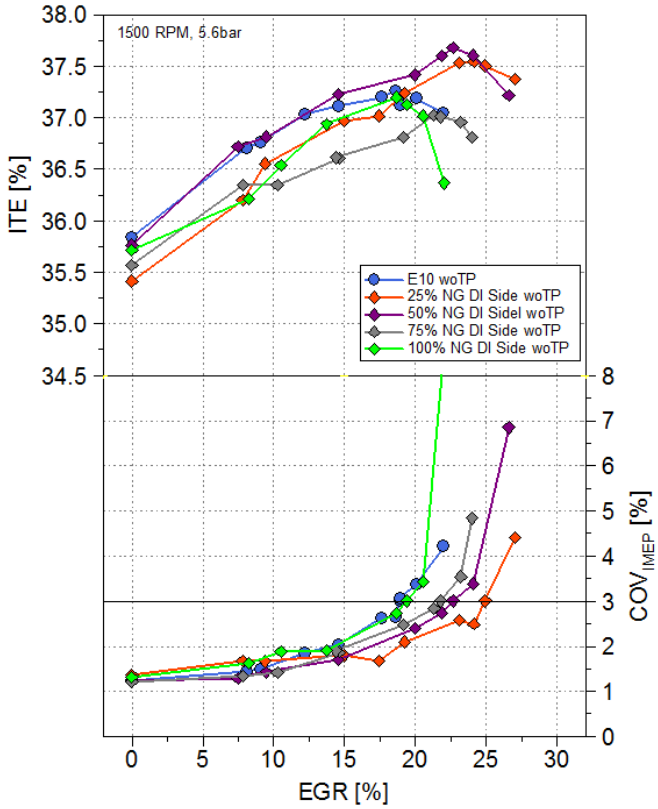

Figure 5: ITE and COVIMEP Versus EGR Dilution Tolerance for NG DI in Side Location, 1500 RPM, 5.6 bar IMEP

Figure 6 shows the engine operation with NG DI in central location and the insert in place. A different relation can be seen in terms of peak efficiency and corresponding COVIMEP. As pure E10 operation was not influenced by the usage of tumble plates, the peak ITE is about 37.7% at 19% EGR dilution tolerance. As the blend ratio was increased, the EGR dilution tolerance increased as well. However, the peak ITE seemed to occur at a COVIMEP lower than 3%, which differs from the trend shown for the engine operation with NG DI in side location. This trend is most striking for higher NG blend ratios such as 75 and 100% NG. As this behavior is most significant for higher blend ratios of NG, a possible increasing disturbance of the homogenous charge with increasing blend ratio could be a conceivable scenario. Additionally, a more stratified charge which produces rich spots close to the cylinder walls and further increases the wall heat transfer could be conceivable.

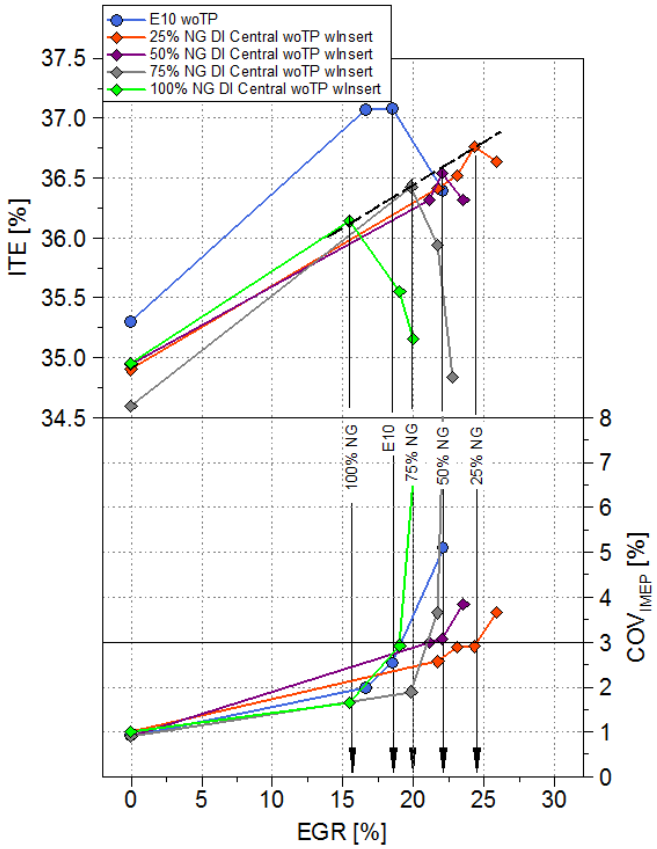

Figure 6: ITE and COVIMEP Versus EGR Dilution Tolerance for NG DI in Central Location, 1500 RPM, 5.6 bar IMEP

Engine Operation with Tumble Plates

In order to study the influence of EGR dilution tolerance and ITE on further increased in-cylinder turbulence levels, tumble plates were installed.

Figure 7 shows the NG DI in side location and NG DI with insert in central location plus tumble plates in place for both engine configurations. The grey lines represent the investigations described in the previous section - engine operation without tumble plates – and serve as a reference compared to the investigations with tumble plates. The biggest differences in EGR dilution tolerance by adding tumble plates can be seen for pure E10 operation, 0% NG. By using tumble plates, the in-cylinder turbulence level was increased compared to the engine operation without tumble plates. As mentioned before, the direct injection event could have possibly contributed to raise the in-cylinder turbulence. Whereas, E10 PFI might not have had such a big impact on in-cylinder turbulence due to the location of the injector and the lower down-stream pressure of only 4 bar compared to 15 bar for the NG DI injection event. In addition, due to the gaseous state of NG under these conditions, the displaced volume is about three orders of magnitude higher when NG is injected compared to the liquid injection of gasoline. The previously mentioned effect is also the cause for the lower volumetric efficiency at WOT for NG PFI compared to E10 PFI. Increasing the blend ratio seems to have only minor impacted the EGR dilution tolerance compared to the change in dilution tolerance with E10 PFI operation. Beyond 25% NG the additional turbulence seemed to increase the EGR dilution tolerance, this trend is most significant for 100% NG. The trend of decreasing EGR dilution tolerance with increasing blend ratio remained. The EGR dilution tolerance for NG DI in side location and NG DI in central location with the insert did not show a difference greater than 1%.

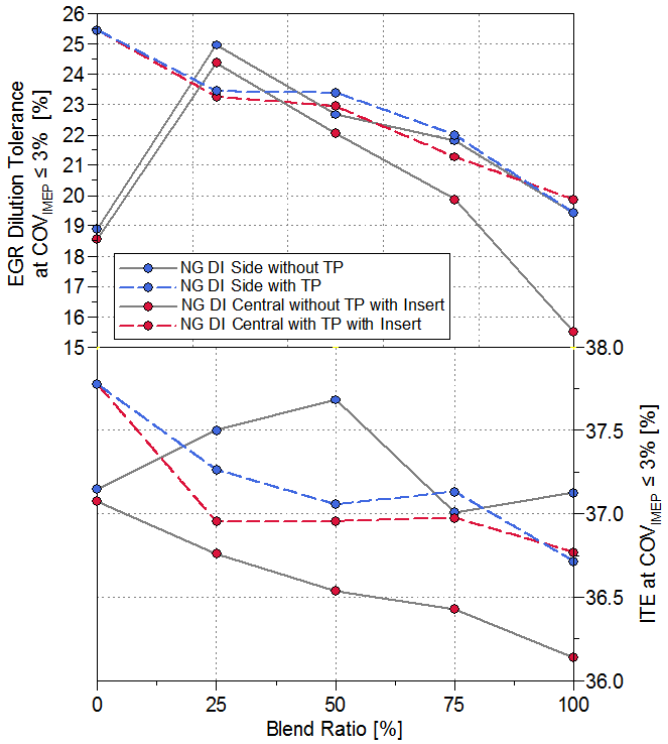

Figure 7: NG DI in Side Location vs NG DI in Central Location with Insert both Fueling Strategies with Tumble Plates Installed, 1500 RPM, 5.6 bar IMEP- EGR

The bottom plot in Figure 7 shows ITE over blend ratio for the investigations with tumble plates. The highest ITE was reached with pure E10 operation, of about 37.8%. Increasing the blend ratio showed a decreasing trend in ITE for both fueling strategies with 100% NG achieving the lowest ITE of about 36.7%. However, a striking fact is the continuously higher ITE for the NG DI operation with the insert in central location. This fueling strategy seemed to benefit from the additional in-cylinder turbulence; possibly due to a better mixing process and more homogenous fuel distribution. Whereas the addition in in-cylinder turbulence seemed to deteriorate the performance for most blend ratios beyond pure E10 operation with the injector in side location. A conceivable scenario could be an increased wall heat transfer with increased turbulence level, as mentioned before.

Comparing the two different engine setups described in the previous section, a different trend in terms of efficiency was seen. The use of tumble plates allowed an increase in efficiency for NG DI in central location, possibly due to an improved mixing process compared to the engine operation without tumble plates. However, NG DI in side location showed a deteriorating efficiency when tumble plates where installed. A conceivable scenario for the decreasing efficiency could be the increasing wall heat transfer with increasing turbulence level. A generally higher efficiency when operating the engine with the NG DI injector in side location was experienced.

Figure 8 shows the trend of ITE and COVIMEP versus EGR dilution tolerance. Significant is the higher ITE of pure E10 operation compared to the other fueling strategies as discussed before. E10 PFI also showed the highest EGR dilution tolerance with about 25%. As seen in the previous section without tumble plates, the peak ITE is reached slightly before or at 3% COVIMEP.

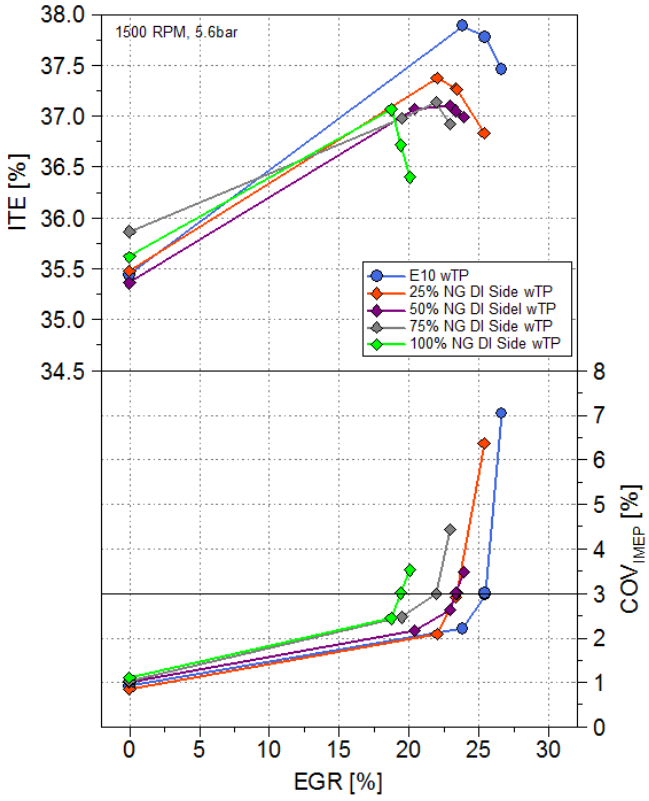

Figure 8:ITE and COVIMEP versus EGR, NG DI in Side Location with Tumble Plates, 1500 RPM, 5.6 bar IMEP

Figure 9 shows ITE and COVIMEP versus EGR rate. Pure E10 showed the same trend as seen as Figure 8 as E10 operation was not influenced by the blended operation with NG in side or central location. When the EGR rate was increased the ITE remained similar from 25% NG up until 75% NG even though the EGR dilution tolerance decreased slightly with increasing EGR rate. A small drop in ITE was experienced with 100% NG operation which also showed the lowest efficiency.

By operating the engine with tumble plates, the performance for pure E10 operation was increased significantly and also the performance for the operation with NG DI in central location and the insert. However, the ITE and EGR dilution tolerance for NG DI in side location deteriorated slightly. The operation with tumble plates showed generally very similar EGR dilution tolerance and ITE for both engine configurations.

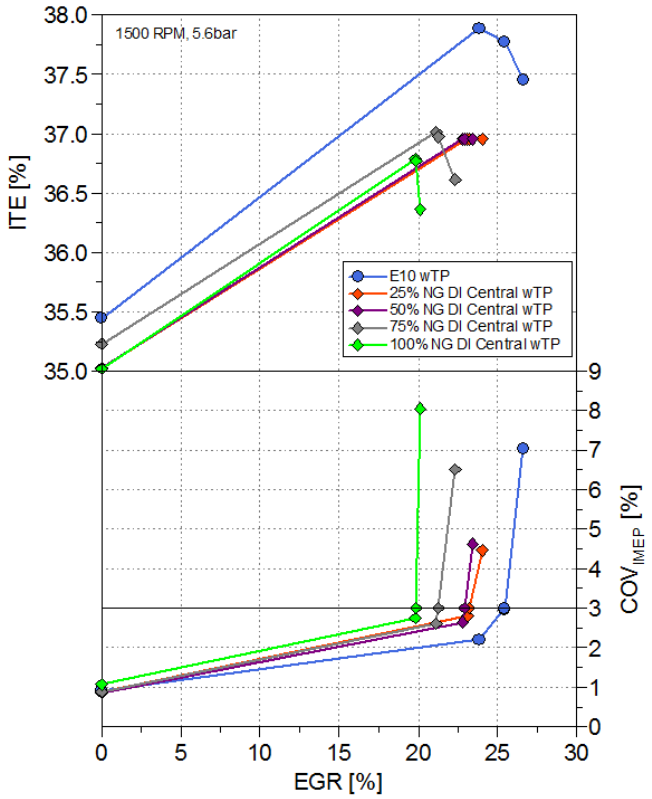

Figure 9:ITE and COVIMEP versus EGR, NG DI in Central Location with Tumble Plates, 1500 RPM, 5.6 bar IMEP

INFLUENCE OF CR ON EGR DILUTION TOLERANCE

For these investigations, there were 3 distinct geometric CR steps tested, 10.5, 12.5 and 14.5. The increase in CR was implemented in order to improve ITE across all engine operation. The first CR step, 12.5, was achieved by lowering the deck height of the engine, which effectively reduced the squish height. The next CR step, 14.5, was achieved by installing a piston with a buildup to reduce the combustion chamber volume at TDC. The squish height for CR 12.5 and 14.5 was the same.

Figure 10 shows the EGR dilution tolerance limit for all five fuel-blending ratios, for the three discrete CR steps. The NG DI SOI was set to 240°CA BTDC because previous research of the authors have shown this to provide the greatest dilution tolerance for this test setup [4]; the E10 PFI SOI was set to 540°CA BTDC. As can be seen, there was a 3.7%abs improvement in the dilution tolerance for E10 operation when going to CR 12.5, likely due to the reduced squish height.

However, at CR 14.5 E10 becomes knock limited for all operation, resulting in a low dilution tolerance. Despite the added diluent, the 50%MFB location for 21.4% EGR condition had to be delayed to 15.7°CA ATDC. 25% NG provided the greatest dilution tolerance; going from CR 10.5 to 12.5 extended the dilution tolerance from 21.1 to 25.0% EGR. The extension of 25% NG is consistent with previous investigations performed at CR 10.5 [6]. Going to CR 14.5 reduced the dilution tolerance to 20.4%. Interestingly enough, as the gasoline fraction was reduced, the dilution tolerance of CR 14.5 became closer in magnitude to the other two CR steps. While the CR 14.5 maintains the same squish height as CR 12.5, it is plausible that the piston buildup causes unfavorable interactions with the in-cylinder charge motion. Literature has shown that a built up piston can lead to a reduction in the tumble motion and turbulence intensity within the cylinder, which would adversely affect dilution tolerance [7]. Consistent with previous findings, there is a decreasing trend in ITE as the blend ratio is increased beyond 25% NG. This decrease in ITE is accompanied by decreasing EGR dilution tolerance. While the gaseous injection event of side has shown to introduce more turbulence, it appears there is a tradeoff between the easier mixture ignitability of E10 and charge motion from side DI. It is also worth mentioning that for most blending conditions, an increase in CR led to an increase in ITE at the 3%COV_{IMEP} level.

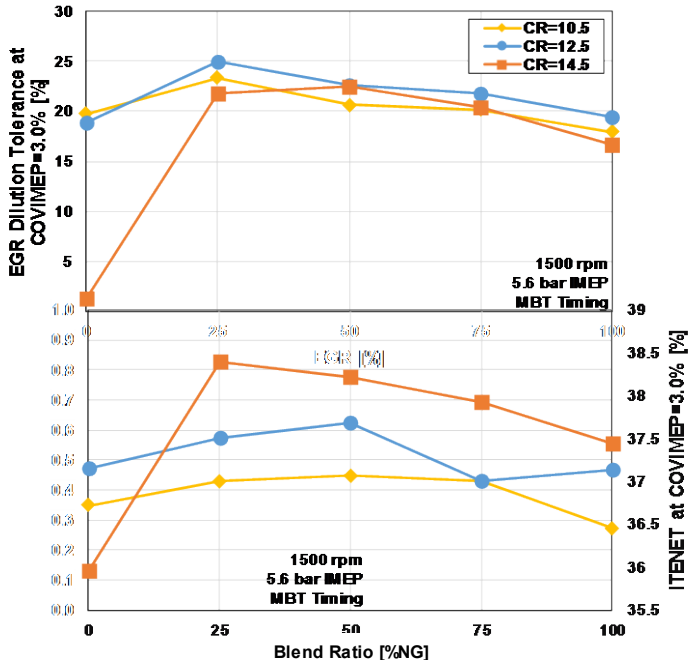

Figure 10: EGR Dilution Tolerance and ITE for all Three CR at Five Fuel Blending Levels

INFLUENCE OF CR ON WOT PERFORMANCE

Increasing the CR in three discrete steps led to interesting findings for natural aspirated WOT performance. The ITE for all three CR steps is shown in Figure 11. For blend ratios 0-50%, CR 10.5 resulted in a higher ITE than CR 12.5; this is because of knock limitations, resulting in a delayed AI50% burn location, seen in Figure 12. Operation with 0 and 25% NG with CR 14.5 was unattainable for this test setup due to severe knocking issues. Delaying the combustion phasing beyond 35°CA ATDC would result in a series of low IMEP cycles, followed by severe knocking cycles because the engine would have too much residual fuel. The highest ITE was seen for 100% NG operation at CR 14.5. Due to the high knock resistance of NG, MBT timing was able to be maintained.

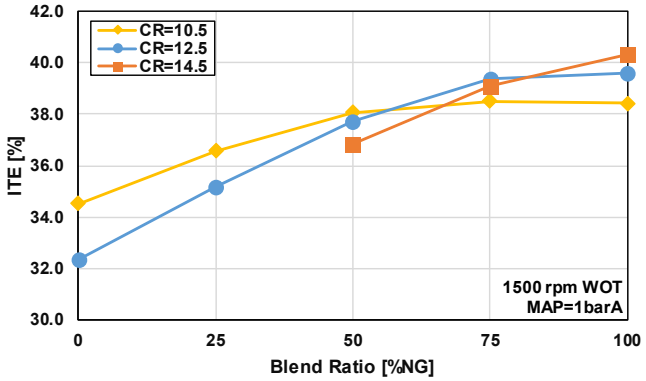

Figure 11: ITE for all Three CR at Five Fuel Blending Levels

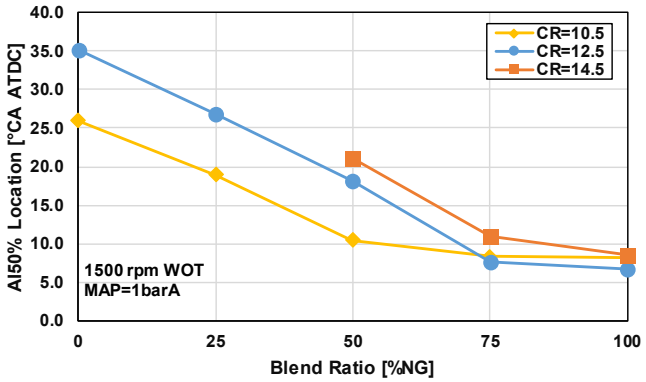

Figure 12: AI50% Burn Location for all Three CR at Five Fuel Blending Levels

Figure 13 shows the IMEP at WOT with MAP set to 1barA. With increasing NG blending ratio, there is a general increase in attainable IMEP. This increase in IMEP is a result of the increasing knock resistance of the blend allowing combustion phasing to be set closer to MBT timing, increasing ITE. At the 100% NG condition, CR 14.5 results in a 1 bar improvement in full load IMEP over CR 10.5. At the same time, this condition also results in a 5% improvement in ITE_{NET}.

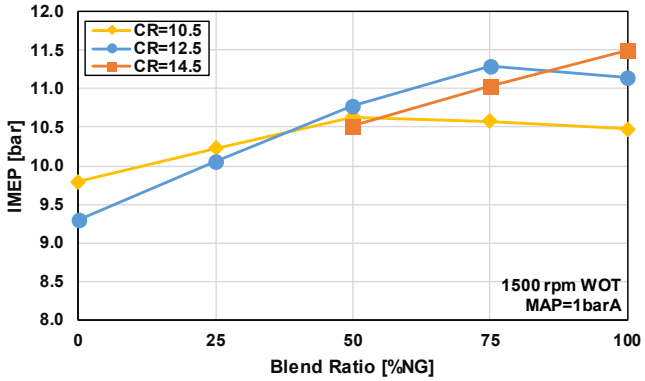

Figure 13: IMEP for all Three CR at Five Fuel Blending Levels

FULL ENGINE MAPS

Full engine maps for all blending levels and all CR steps are shown in Figure 14 through Figure 18.

For E10 operation, shown in Figure 14, similar efficiencies were achieved in part-load conditions with EGR, regardless of CR. For the case of CR 12.5 and 14.5, additional EGR helped to reduce the propensity to knock. It is worth mentioning, engine operation at CR 12.5 becomes knock limited beyond 5.6 bar IMEP regardless of engine speed. The highest efficiencies at WOT were achieved at CR 10.5. Increasing the CR beyond that resulted in a penalty for efficiency and IMEP at WOT due to knocking combustion necessitating delayed combustion phasing. For CR 10.5 and 12.5, full engine operation could be attained despite requiring delayed combustion. At 1500 RPM, increasing to CR 12.5 resulted in a 2.1% loss in efficiency and 3 bar loss in IMEP. At CR 14.5, 8bar and WOT was not attainable due to severe knock limitations. Operation at CR 12.5 had already become knock limited at the 8 bar condition.

Figure 15 shows the engine operation for 25% NG at CR 10.5, 12.5, and 14.5. Increasing the blend ratio led similar part-load efficiencies as E10 for all CR levels. The benefit of 25% NG was noticed at 8 bar and WOT. For the case of CR 12.5, blending 25% NG at 2000 RPM WOT, the IMEP was able to be increased to 11 bar and efficiency from 29.1 to 36.7%, relative to CR 10.5. However, with 25% NG, delayed phasing was still required for WOT CR 10.5 and 12.5. With the addition of 25% NG, engine load for CR 14.5 was able to be increased to 8 bar IMEP, despite requiring delayed phasing.

Engine maps for 50% NG are shown in Figure 16. Consistent with previous CR steps, similar efficiency levels are attained at the part-load conditions. At CR10.5, 50% NG is required to maintain MBT timing without knocking combustion. However, knocking combustion still occurred at WOT for CR 12.5 and 14.5, requiring delayed combustion phasing. 50% NG is the first instance where full engine operation can be attained for CR 14.5. Consequently, the potential efficiency improvements due to CR 14.5 are still not realized due to delayed combustion phasing. In fact, CR 10.5 still attains higher efficiency at WOT relative to CR 14.5.

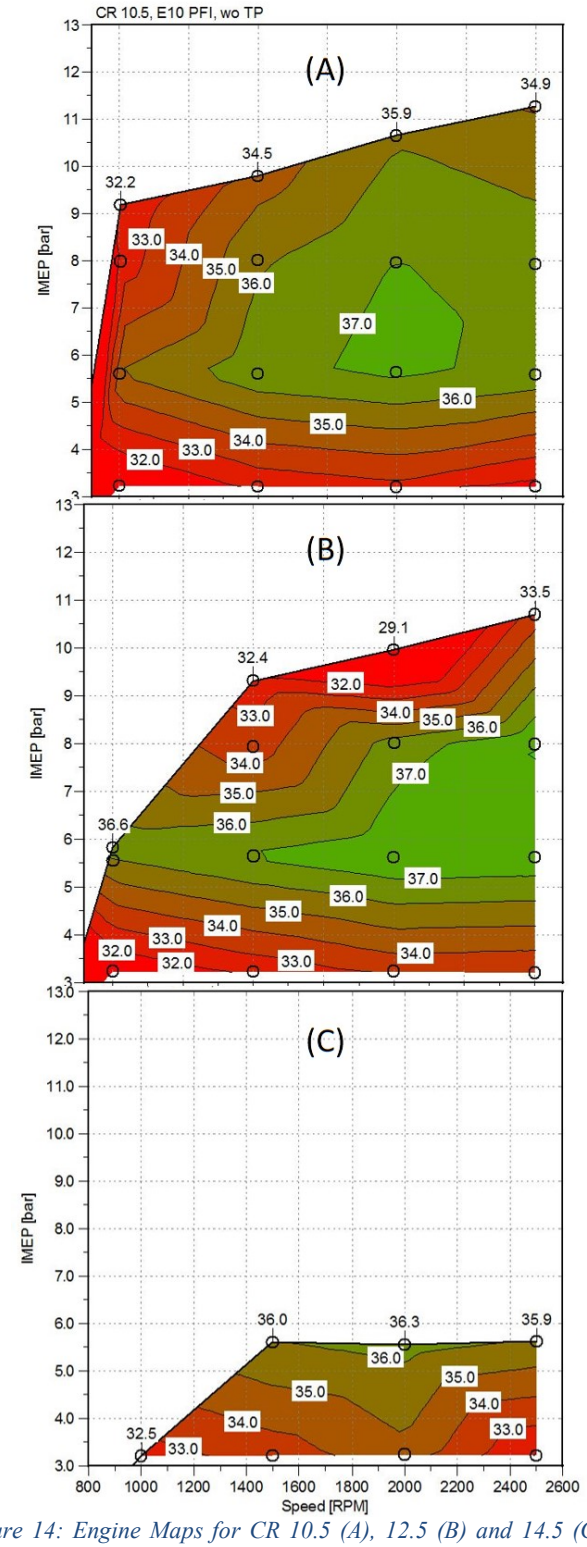

Figure 14: Engine Maps for CR 10.5 (A), 12.5 (B) and 14.5 (C) for E10 Operation

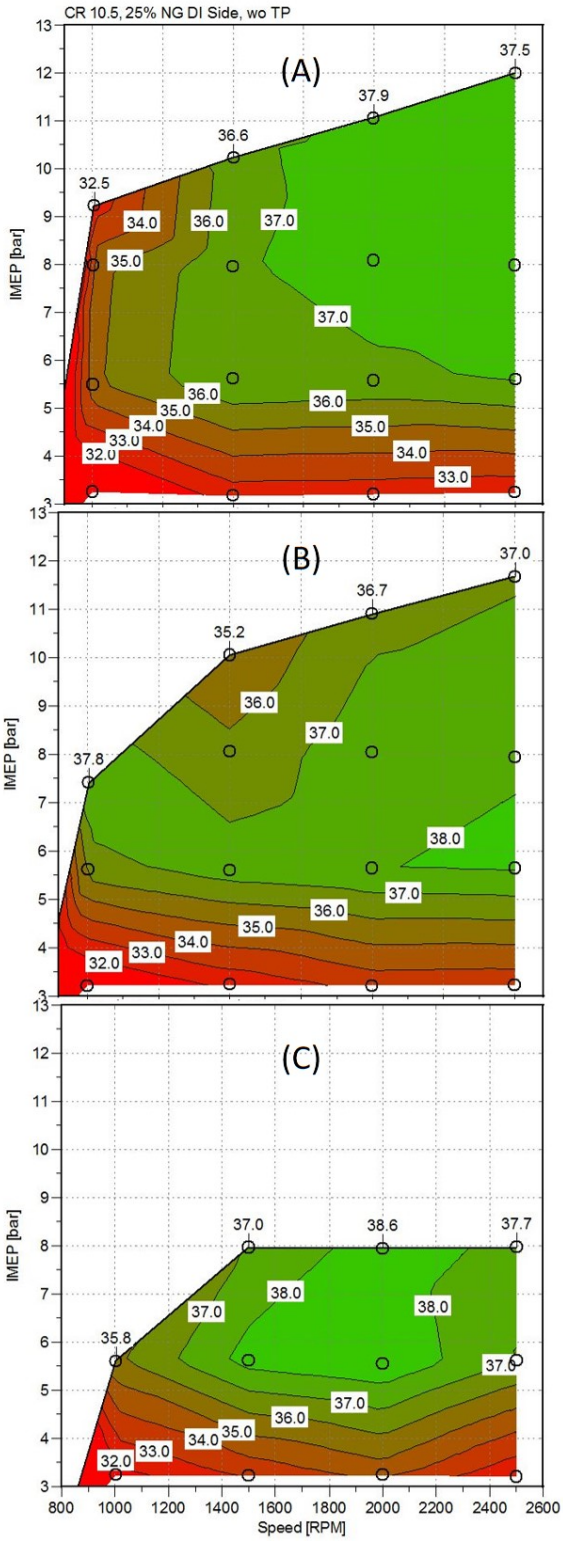

Figure 15: Engine Maps for CR 10.5 (A), 12.5 (B) and 14.5 (C) for 25% NG Operation

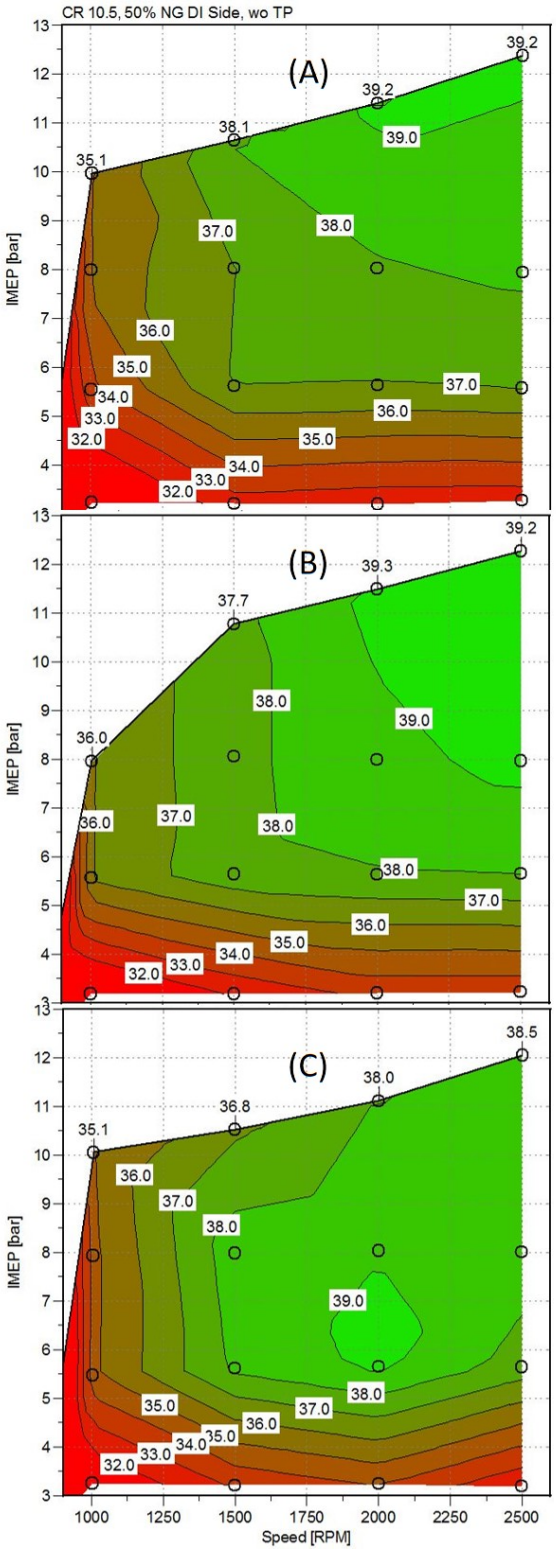

Figure 16: Engine Maps for CR 10.5 (A), 12.5 (B) and 14.5 (C) for 50% NG Operation

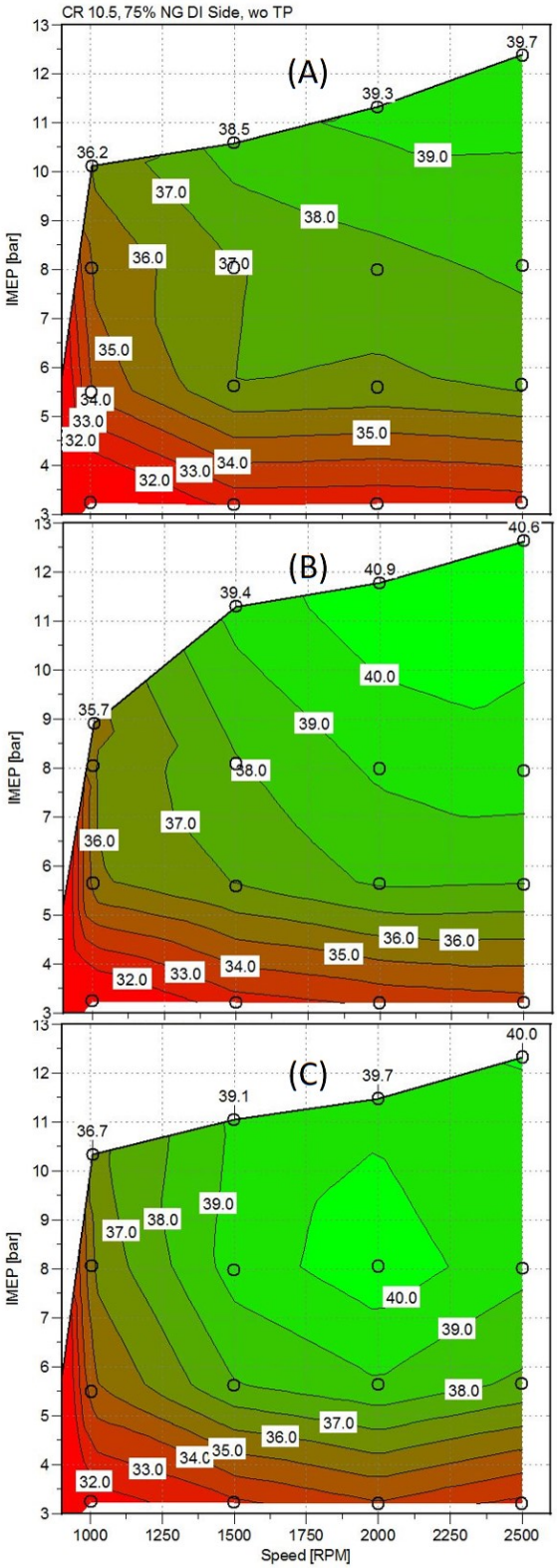

Figure 17: Engine Maps for CR 10.5 (A), 12.5 (B) and 14.5 (C) for 75% NG Operation

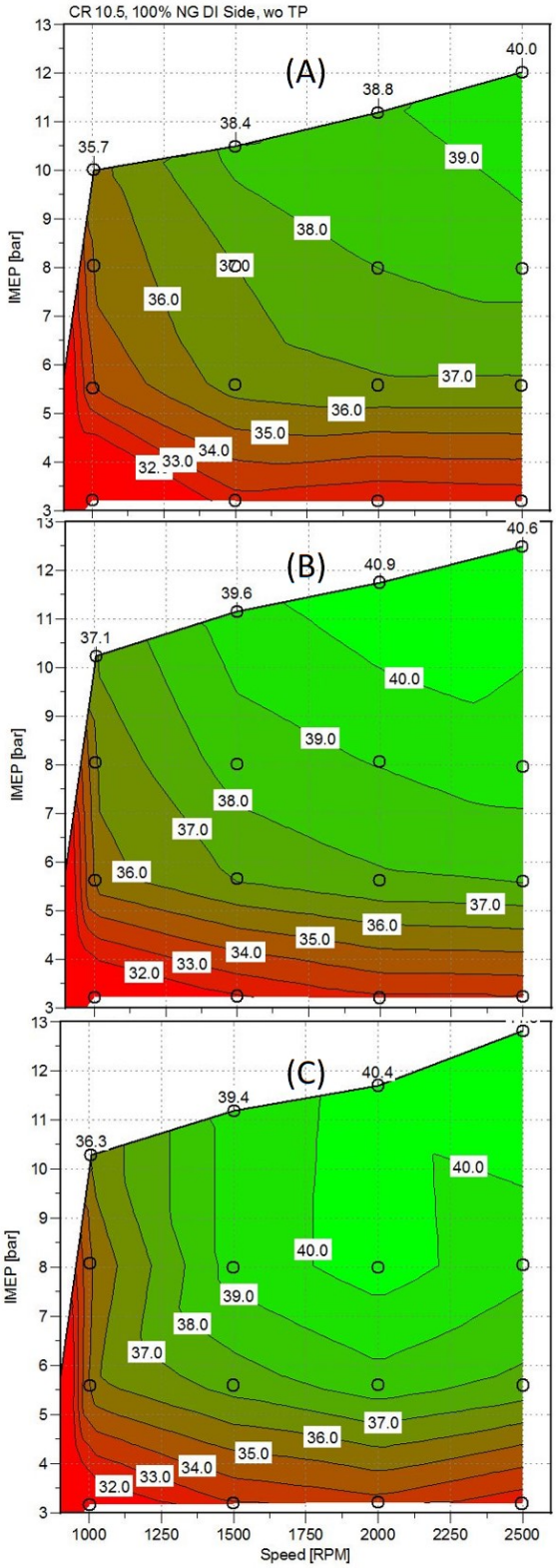

Figure 18: Engine Maps for CR 10.5 (A), 12.5 (B) and 14.5 (C) for 100% NG Operation

Operation with 75% NG is shown in Figure 17. Looking at CR 10.5, there were marginal improvements in efficiency at WOT over 50% NG operation. However, at CR 12.5, there was a 2.4% improvement in efficiency at 1500 RPM WOT as well as up to a 0.5 bar improvement in IMEP. The added benefits of CR 14.5 start to become apparent at 75% NG. Operation beyond 8 bar IMEP at 1000 RPM is attainable with 75% NG, allowing for an engine load of 10.3 bar and efficiency of 36.7%.

Engine operation for 100% NG is shown in Figure 18. Regardless of CR, 100% NG is the only fueling strategy that allows for knock free combustion. Once again, similar efficiencies were realized at part-load conditions. For CR 12.5 and 14.5 there were similar efficiencies at WOT. It is conceivable an efficiency gain was not realized for CR 14.5 due to the higher surface to volume ratio with the domed piston, leading to higher heat transfer losses. However, at the 2500 RPM WOT case, CR 14.5 allowed for up to a 0.3 bar improvement in IMEP.

As seen in Figure 14, E10 operation becomes severely limited for the elevated CR steps. The operating range of the engine increased with increasing NG content. As it appears, CR 12.5 is optimal for this test setup, allowing for full engine operation on all fuel blends, while also yielding an efficiency benefit relative to the CR 10.5 baseline. While it is true CR 14.5 would lead to higher efficiency levels, fuel engine operation is only available for 60% of the fueling strategies investigated.

CONCLUSION

As shown, there were several methods utilized to improve the efficiency, dilution tolerance, and full load potential of an engine using NG DI as well as hardware techniques. With the injector in the central location and utilizing an insert, the dilution tolerance under blended operation was able to be similar to side mounted injection. However, there was an efficiency penalty possibly due to increased wall heat transfer. The use of port blocking tumble plates to increase the tumble motion had the greatest impact when operating with PFI. With NG DI, the central location yielded the greatest efficiency improvement, possibly due to improve turbulence and mixing. The side location did not yield a benefit, likely due to the increase turbulence increasing wall heat transfer.

Increasing the CR led to an improvement in dilution tolerance and resulting efficiency. The greatest dilution tolerance was achieved with CR 12.5 due to the reduce squish height. A dilution tolerance penalty occurred for CR 14.5 likely due to the domed piston reducing some of the in-cylinder turbulence at the time of spark.

As can be seen, there are multiple means to improve the dilution tolerance and efficiency of the engine. For this test setup, there is an optimal hardware configuration in order to yield the best operating range on all fuel blends and the resulting efficiency. Injection in the side location resulted in the greatest tradeoff between dilution tolerance and resulting efficiency. For the case of side DI, introducing tumble plates did not provide any benefit; in fact, for the case of 25% NG, the tumble plates reduced the dilution tolerance. In addition, the tumble plates would have resulted in a power density loss for side DI. When considering full engine operation for all blend ratios, CR 12.5 provides the best benefit.

ACKNOWLEDGMENTS

The submitted manuscript has been created by UChicago Argonne, LLC, Operator of Argonne National Laboratory (“Argonne”). Argonne, a U.S. Department of Energy Office of Science laboratory, is operated under Contract No. DE-AC02-06CH11357. The U.S. Government retains for itself, and others acting on its behalf, a paid-up nonexclusive, irrevocable worldwide license in said article to reproduce, prepare derivative works, distribute copies to the public, and perform publicly and display publicly, by or on behalf of the Government.
This research is funded by DOE's Vehicle Technologies Program, Office of Energy Efficiency and Renewable Energy through an award based on the FY 2014 Vehicle Technologies Program Wide Funding Opportunity Announcement DE-FOA-0000991 (0991-1822). The authors would like to express their gratitude to Kevin Stork, program manager at DOE, for his support.

REFERENCES

[1] Sevik, J., Pamminger, M., Wallner, T., Scarcelli, R. et al., "Performance, Efficiency and Emissions Assessment of Natural Gas Direct Injection compared to Gasoline and Natural Gas Port-Fuel Injection in an Automotive Engine," SAE Int. J. Engines 9(2):1130-1142, 2016, doi:10.4271/2016-01-0806.
[2] Husted, H., Karl, G., Schilling, S.,Weber, C., “Direct Injection of CNG for Driving Performance with Low CO2,” 23rd Aachen Colloquium Automobile and Engine Technology 2014.
[3] "Crank Angle Encoder of 365-Series." Crank Angle Encoder of 365-Series - Combustion Measurement. N.p., n.d. Web. 28 Apr. 2017.
[4] Sevik, J., Pamminger, M., Wallner, T., Scarcelli, R. et al., "Influence of Injector Location on Part-Load Performance Characteristics of Natural Gas Direct-Injection in a Spark Ignition Engine," SAE Int. J. Engines 9(4):2262-2271, 2016, doi:10.4271/2016-01-2364.
[5] Heywood, J.B., "Internal Combustion Engine Fundamentals," McGraw-Hill Book.
[6] Pamminger, M., Wallner, T., Sevik, J., Scarcelli, R. et al., “Performance, Efficiency and Emissions Evaluation of Gasoline Port-Fuel Injection, Natural Gas Direct Injection and Blended Operation”, ASME ICEF 2016, ICEF2016-9370.
[7] Iyer, C. and Yi, J., "3D CFD Upfront Optimization of the In-Cylinder Flow of the 3.5L V6 EcoBoost Engine," SAE Technical Paper 2009-01-1492, 2009, doi:10.4271/2009-01-1492.

NOMENCLATURE

AI	Area integrated
ATDC	After top dead center
BTDC	Before top dead center
CD	Combustion duration
CFD	Computational fluid dynamics
CO2	Carbon dioxide
COV	Coefficient of variance
CR	Compression ratio
DI	Direct injection
EGR	Exhaust gas recirculation
EVO	Exhaust valve opening
FDA	Flame development angle
IMEP	Indicated mean effective pressure
ITE	Indicated thermal efficiency
IVC	Intake valve closing
NG	Natural gas
PFI	Port-fuel injection
SOI	Start of injection
ST	Spark timing
TP	Tumble plates
WOT	Wide open throttle

1 Sevik, J., Pamminger, M., Wallner, T., Scarcelli, R. et al., "Performance, Efficiency and Emissions Assessment of Natural Gas Direct Injection compared to Gasoline and Natural Gas Port-Fuel Injection in an Automotive Engine," SAE Int. J. Engines 9(2):1130-1142, 2016, doi:10.4271/2016-01-0806.
2 Husted, H., Karl, G., Schilling, S.,Weber, C., “Direct Injection of CNG for Driving Performance with Low CO2,” 23rd Aachen Colloquium Automobile and Engine Technology 2014.
3 "Crank Angle Encoder of 365-Series." Crank Angle Encoder of 365-Series - Combustion Measurement. N.p., n.d. Web. 28 Apr. 2017.
4 Sevik, J., Pamminger, M., Wallner, T., Scarcelli, R. et al., "Influence of Injector Location on Part-Load Performance Characteristics of Natural Gas Direct-Injection in a Spark Ignition Engine," SAE Int. J. Engines 9(4):2262-2271, 2016, doi:10.4271/2016-01-2364.
5 Heywood, J.B., "Internal Combustion Engine Fundamentals," McGraw-Hill Book.
6 Pamminger, M., Wallner, T., Sevik, J., Scarcelli, R. et al., “Performance, Efficiency and Emissions Evaluation of Gasoline Port-Fuel Injection, Natural Gas Direct Injection and Blended Operation”, ASME ICEF 2016, ICEF2016-9370.
7 Iyer, C. and Yi, J., "3D CFD Upfront Optimization of the In-Cylinder Flow of the 3.5L V6 EcoBoost Engine," SAE Technical Paper 2009-01-1492, 2009, doi:10.4271/2009-01-1492.